References and Notes

1. M. A. Brzezinski *et al.*, *Geophys. Res. Lett.* **29**, 1564 (2002).
2. K. Matsumoto, J. L. Sarmiento, M. A. Brzezinski, *Global Biogeochem. Cycles* **16**, 1031 (2002).
3. S. Takeda, *Nature* **393**, 774 (1998).
4. J. L. Sarmiento, N. Gruber, M. A. Brzezinski, J. P. Dunne, *Nature* **427**, 56 (2004).
5. J. L. Sarmiento *et al.*, *Global Biogeochem. Cycles* **21**, GB1S90 (2007).
6. Y. Rosenthal, E. A. Boyle, L. Labeyrie, *Paleoceanography* **12**, 787 (1997).
7. U. S. Ninnemann, C. D. Charles, *Earth Planet. Sci. Lett.* **201**, 383 (2002).
8. D. A. Hodell, K. A. Venz, C. D. Charles, U. S. Ninnemann, *Geochem. Geophys. Geosyst.* **4**, 1004 (2003).
9. E. A. Boyle, *Annu. Rev. Earth Planet. Sci.* **20**, 245 (1992).
10. L. C. Skinner, S. Fallon, C. Waelbroeck, E. Michel, S. Barker, *Science* **328**, 1147 (2010).
11. A. D. Moy, W. R. Howard, M. K. Gagan, *J. Quat. Sci.* **21**, 763 (2006).
12. I. N. McCave, L. Carter, I. R. Hall, *Quat. Sci. Rev.* **27**, 1886 (2008).
13. U. S. Ninnemann, C. D. Charles, *Paleoceanography* **12**, 560 (1997).
14. A. M. Piotrowski, S. L. Goldstein, S. R. Hemming, R. G. Fairbanks, *Earth Planet. Sci. Lett.* **225**, 205 (2004).
15. K. R. Hendry, R. B. Georg, R. E. M. Rickaby, L. F. Robinson, A. N. Halliday, *Earth Planet. Sci. Lett.* **292**, 290 (2010).
16. C. L. de la Rocha, M. A. Brzezinski, M. J. DeNiro, *Geochim. Cosmochim. Acta* **61**, 5051 (1997).
17. M. Wille *et al.*, *Earth Planet. Sci. Lett.* **292**, 281 (2010).
18. See the supporting online material available on *Science* Online.
19. D. W. Lea, *Paleoceanography* **10**, 733 (1995).
20. R. F. Anderson *et al.*, *Science* **323**, 1443 (2009).
21. S. Barker *et al.*, *Nature* **457**, 1097 (2009).
22. Z. Chase, R. F. Anderson, M. Q. Fleisher, P. W. Kubik, *Deep Sea Res. Part II Top. Stud. Oceanogr.* **50**, 799 (2003).
23. R. B. Georg, A. J. West, A. R. Basu, A. N. Halliday, *Earth Planet. Sci. Lett.* **283**, 67 (2009).
24. P. N. Froelich *et al.*, *Paleoceanography* **7**, 739 (1992).
25. M. J. Ellwood, M. Kelly, W. A. Maher, P. De Deckker, *Earth Planet. Sci. Lett.* **243**, 749 (2006).
26. C. L. De La Rocha, M. A. Brzezinski, M. J. DeNiro, A. Shemesh, *Nature* **395**, 680 (1998).
27. L. E. Pichevin *et al.*, *Nature* **459**, 1114 (2009).
28. D. M. Sigman, M. P. Hain, G. H. Haug, *Nature* **466**, 47 (2010).
29. D. A. Hodell *et al.*, in *Proceedings of the Ocean Drilling Program, Scientific Results Volume*, R. Gersonde, D. A. Hodell, P. Blum, Eds. (Ocean Drilling Program, College Station, TX, 2002), vol. 177.
30. R. A. Mortlock *et al.*, *Nature* **351**, 220 (1991).

31. We acknowledge the Antarctic Research Facility at Florida State University for E33-22 core samples and the Ocean Drilling Program for ODP177 site 1089 core samples. This research was supported with funds from the Australian Research Council (grants DP0770820 and DP0771519). This manuscript benefited from the thoughtful comments of two anonymous reviewers.

Supporting Online Material

www.sciencemag.org/cgi/content/full/science.1194614/DC1
Materials and Methods
SOM Text
Figs. S1 to S7
Tables S1 to S4
References

2 July 2010; accepted 28 September 2010
Published online 21 October 2010;
10.1126/science.1194614

Structure of the Human Dopamine D3 Receptor in Complex with a D2/D3 Selective Antagonist

Ellen Y. T. Chien,[1] Wei Liu,[1] Qiang Zhao,[1] Vsevolod Katritch,[2] Gye Won Han,[1] Michael A. Hanson,[3] Lei Shi,[4] Amy Hauck Newman,[5] Jonathan A. Javitch,[6] Vadim Cherezov,[1] Raymond C. Stevens[1]*

Dopamine modulates movement, cognition, and emotion through activation of dopamine G protein–coupled receptors in the brain. The crystal structure of the human dopamine D3 receptor (D3R) in complex with the small molecule D2R/D3R-specific antagonist eticlopride reveals important features of the ligand binding pocket and extracellular loops. On the intracellular side of the receptor, a locked conformation of the ionic lock and two distinctly different conformations of intracellular loop 2 are observed. Docking of R-22, a D3R-selective antagonist, reveals an extracellular extension of the eticlopride binding site that comprises a second binding pocket for the aryl amide of R-22, which differs between the highly homologous D2R and D3R. This difference provides direction to the design of D3R-selective agents for treating drug abuse and other neuropsychiatric indications.

Dopamine is an essential neurotransmitter in the central nervous system and exerts its effects through activation of five distinct dopamine receptor subtypes that belong to the G protein–coupled receptor (GPCR) superfamily. The receptors have been classified into two subfamilies, D1-like and D2-like, on the basis of their sequence and pharmacological similarities (*1*). The D1-like receptors (D1R and D5R) couple to stimulatory G-protein α subunits ($G_{s/olf}$), activating adenyl cyclase, whereas D2-like receptors (D2R, D3R, and D4R) couple to inhibitory G-protein α subunits ($G_{i/o}$), inhibiting adenyl cyclase. The high degree of sequence identity (*2*, *3*) within the transmembrane (TM) helices between D2R and D3R (78%), and more importantly, the near-identity of the residues inferred to form the binding site in these receptors (*4*), have created a formidable challenge to developing D3R-selective compounds with drug-like physicochemical properties (*3*, *5*). Antipsychotic drugs that block both D2R and D3R are used clinically to treat schizophrenia, but these agents can produce multiple side effects that can limit their tolerability. It has been hypothesized that selective targeting of the individual D2-like receptor subtypes might produce fewer side effects (*6*). Through extensive medicinal chemistry efforts, D3R-preferential antagonists and partial agonists (e.g., SB 277011A, NGB 2904, BP 897; see fig. S1) have been developed and shown to attenuate drug-seeking behaviors in animal models of relapse, without associated motor effects, supporting D3R blockade as a plausible target for therapeutic discovery (*7*–*11*) particularly for substance abuse (*12*). However, even the best D3R-preferential compounds are still highly lipophilic and display poor bioavailability or predicted toxicity that has precluded clinical trials. To better understand dopamine receptors and the molecular basis for pharmacological specificity within the dopamine receptors, we have determined the crystal structure of the human D3R in complex with eticlopride, a potent D2R/D3R antagonist (*13*, *14*).

To crystallize the D3R, we modified it by introducing a point mutation in the transmembrane domain [Leu119$^{3.41}$Trp (*15*)] to enhance thermal stability (*16*), and replacing most of the third cytoplasmic loop (ICL3) (Arg222 to Arg318) with T4-lysozyme (D3R-T4L) (*17*). Further stabilization of the receptor was achieved by purifying with the antagonist eticlopride, which conferred the highest thermostability compared with five other ligands (*18*) (table S2). The engineered receptor retained near-native ligand binding properties (table S3) and crystallized from a lipidic mesophase in an orthorhombic space group. Diffraction data were anisotropic, extending to 2.9 Å in the *c** direction and 3.6 Å in the *a** direction. Overall, the structure was determined at 3.15 Å and included all data up to 2.9 Å where an improvement in map quality was observed (see fig. S8 and table S1). The structure was determined with two receptors arranged in an antiparallel orientation in the asymmetric unit of the crystal (fig. S2). Both copies of the receptor are very similar [root mean square deviation of 0.6 Å for the seven-TM bundle] and will be treated identically in the discussion

[1]Department of Molecular Biology, The Scripps Research Institute, 10550 North Torrey Pines Road, La Jolla, CA 92037, USA. [2]Skaggs School of Pharmacy and Pharmaceutical Sciences, and San Diego Supercomputer Center, University of California, San Diego, La Jolla, CA 92093, USA. [3]Receptos, 10835 Road to the Cure, Suite 205, San Diego, CA 92121, USA. [4]Department of Physiology and Biophysics and HRH Prince Alwaleed Bin Talal Bin Abdulaziz Alsaud Institute for Computational Biomedicine, Weill Cornell Medical College, Cornell University, 1300 York Avenue, New York, NY 10021, USA. [5]Medicinal Chemistry Section, National Institute on Drug Abuse–Intramural Research Program, Baltimore, MD 21224, USA. [6]Center for Molecular Recognition and Departments of Psychiatry and Pharmacology, Columbia University College of Physicians and Surgeons, 630 West 168th, New York, NY 10032, USA.

*To whom correspondence should be addressed. E-mail: stevens@scripps.edu

Downloaded from www.sciencemag.org on October 15, 2015

except where noted otherwise. The N-terminal 31 residues are not included in the deposited structure as they do not have interpretable density. The main fold of the D3R consists of the canonical seven-TM bundle of α helices (Fig. 1A), which resembles previously solved GPCR structures (*19*–*22*). Subtleties in the orientations of these helices, as well as differences in the intracellular and extracellular portions of the receptor, confer the pharmacological and biochemical properties unique to the D3R.

The extracellular region in general is characterized by high sequence diversity among the GPCR family, which translates into high structural diversity in terms of the presence of varied secondary-structure elements and the presentation of individual amino acids in the binding pocket (*23*, *24*). In the D2R and D3R, for instance, the second extracellular loop (ECL2) is much shorter than in the β-adrenergic receptors (βARs) and lacks the helical secondary structure. The portion of ECL2 in D3R (residues 182 to 185) that contributes to the ligand binding pocket is quite similar to that in the βARs in both spatial positioning relative to bound ligand, and in the presentation of side chains in the ligand binding pocket. In the D3R, a disulfide bond is formed between Cys355 and Cys358 in ECL3 in addition to the canonical disulfide bond bridging ECL2 (Cys181) and helix III ($Cys103^{3.25}$) (*25*). Comparison of the D3R structure to the β_2AR structure reveals small shifts in the helical bundle; for example, the extracellular tips of helices VI and VII are tilted by ~3 Å and ~2 Å, respectively (Fig. 1B), whereas the extracellular tips of helices III and V are about 3.5 Å closer to each other in the D3R as compared with the β_2AR structure. The latter shift can be explained by the fact that a segment of ECL2 connecting the tips of helixes V and III through a C181-$Cys103^{3.25}$ disulfide bond in D3R and other D2-like receptors is one amino acid shorter than in β_2AR and D1-like dopamine receptors (see fig. S4, B and D).

A common feature thought to be important in many class A GPCRs is the ionic lock—a salt bridge between the charged $Arg^{3.50}$ in the conserved "D[E]RY" motif and $Asp/Glu^{6.30}$ at the cytoplasmic side of helices III and VI. This interaction is observed in all of the inactive rhodopsin crystal structures (Fig. 2A) (*26*, *27*) and has been implicated through mutagenesis as a major factor in stabilizing the receptors in the inactive conformation (*28*, *29*). Despite the presence of residues capable of forming this interaction, the ionic lock has not been found in any of the other GPCR crystal structures published to date (*19*–*22*) (Fig. 2, C to E). The absence of this interaction is puzzling given its presumed importance and has been thought to be partly attributable to the inclusion of the T4L fusion protein within ICL3, which may induce a non-native helical conformation within this region. However, the presence of an intact ionic lock in both molecules in the D3R structure establishes the possibility of forming this interaction in the presence of T4L (Fig. 2B). The propensity for formation of the ionic lock, therefore, may indicate different distributions of conformational states in different receptors that may have direct implications for basal signaling activities. Differences between the two molecules observed in the crystallographic asymmetric unit may highlight particular areas of conformational flexibility in receptor structure. In chain A, ICL2 forms a 2.5 turn α helix that runs parallel to the membrane (Fig. 1A). The observation of this α

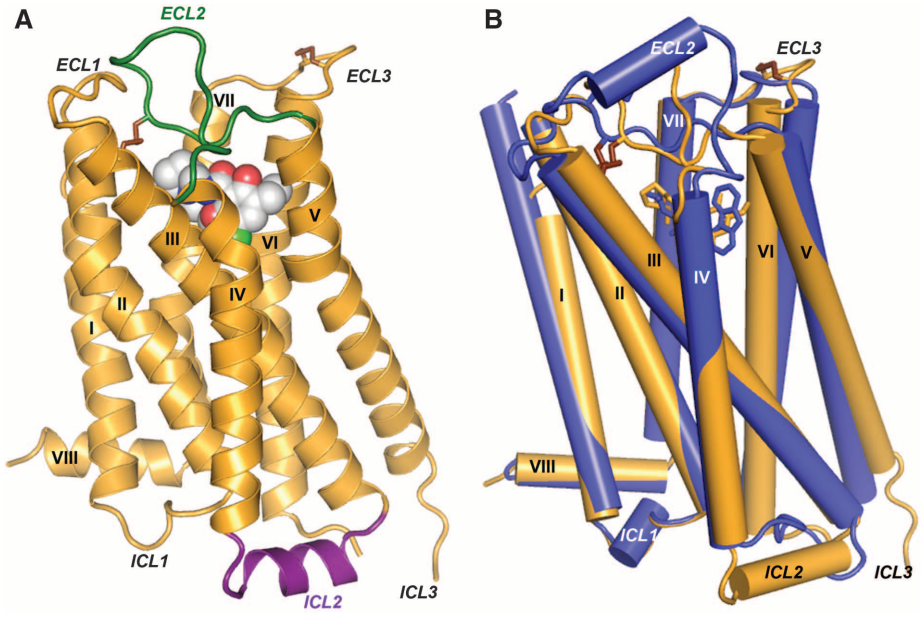

Fig. 1. Overall D3R structure with eticlopride and comparison with β_2AR structure. (**A**) A model of the D3R with the bound ligand eticlopride in space-filling representation; ECL2 is shown in green, ICL2 in purple, and disulfide bonds in brown (conformation of chain A shown). (**B**) Comparison of the TM domains of D3R (brown) and β_2AR (blue; PDB ID: 2RH1).

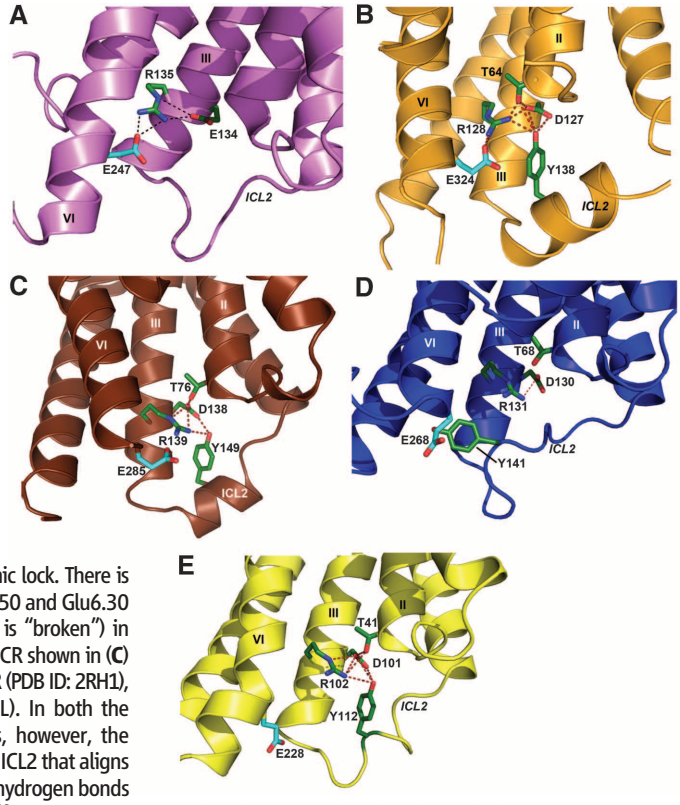

Fig. 2. Conformation of ICL2 and ionic lock motif in D3R and other GPCR structures. As also seen in (**A**) the inactive Rhodopsin structure (PDB ID: 1U19), the conserved ionic lock motif D[E]RY is in a "locked" conformation in (**B**) the D3R structure, i.e., with a salt bridge formed between $Arg128^{3.50}$ and $Glu324^{6.30}$. In addition, the side chain of Tyr138 in the ICL2 α helix of the D3R is inserted into the seven-TM bundle forming hydrogen bonds with $Thr64^{2.39}$, $Arg128^{3.50}$, and $Asp127^{3.49}$ (distances of 3.0, 3.2, and 3.2 Å, respectively), potentially stabilizing the ionic lock. There is no salt bridge between Arg3.50 and Glu6.30 (and hence the "ionic lock" is "broken") in other crystal structures of GPCR shown in (**C**) β_1AR (PDB ID: 2VT4), (**D**) β_2AR (PDB ID: 2RH1), and (**E**) A_{2A}AR (PDB ID: 3EML). In both the β_1AR and A_{2A}AR structures, however, the corresponding Tyr residue in ICL2 that aligns to Tyr138 in D3R forms two hydrogen bonds with the $Asp^{3.49}$ and $Arg^{3.50}$ side chains even in the absence of the closed ionic lock conformation. Salt bridges and hydrogen bond interactions are shown as dashed lines.

helix in only one copy of the receptor may be due to the conformational dynamics of ICL2 and the associated regions (*30*), as in chain B, ICL2 is unstructured and the intracellular ends of helices IV and V are shifted ~2.9 Å closer to each other relative to their positions in chain A (fig. S3C). The two different conformational states of ICL2 observed in the D3R structure suggest that this helix is transient, raising the possibility that interactions between ICL2 and the receptor ionic lock may modulate the signaling properties of the D3R and perhaps contribute to the tolerance property in D3R signaling that persists after agonist is removed (*31*).

Strong electron density was observed for eticlopride in the binding cavity (fig. S3, A and B), which is similar to the β_2AR pocket (Fig. 3, C and D), as expected for receptors that bind closely related catecholamine ligands (*32*). The similarity includes a number of conserved side chains in the core binding site deep in the seven-TM bundle (10 of 18 eticlopride contact residues are conserved in the β_2AR) and open access to this site through a crevice from the extracellular side. Compared with the β_2AR, however, a part of the D3R access crevice is blocked by the inward shift of helices V and VI, and access to the ligand binding pocket is controlled by side chains of helices I, II, III, VII, and ECL2.

Eticlopride occupies the part of the binding pocket defined by side chains from helices II, III, V, VI, and VII (Figs. 1 and 3A and table S4) that largely overlaps with the carazolol binding site in the β_2AR (Fig. 1B). The tertiary amine in the ethyl-pyrrolidine ring of eticlopride is likely charged at physiological pH and forms a salt bridge (2.8 Å) to the carboxylate of Asp110$^{3.32}$, which is highly conserved in all aminergic receptors (Fig. 3, A and B). This salt bridge is structurally and pharmacologically critical for high-affinity ligand binding to the aminergic subfamily of GPCRs (*4*, *33*). Another key component of the eticlopride pharmacophore is a substituted aromatic ring connected to the pyrrolidine by an amide bond that fits tightly within a hydrophobic cavity formed by Phe345$^{6.51}$ and Phe346$^{6.52}$ in helix VI; Val189$^{5.39}$, Ser192$^{5.42}$, and Ser193$^{5.43}$ in helix V; and Val111$^{3.33}$ in helix III, as well as Ile183 in ECL2. Polar substituents (e.g., OH, OCH_3) in the phenyl ring form intramolecular hydrogen bonds with both the N and O of the amide, thereby maintaining the compound in an almost planar conformation (Fig. 3, A and B), consistent with the small-molecule crystal structure determination (*13*).

Of the 18 eticlopride contact residues in the D3R structure, 17 are identical in the D2R (Val350$^{6.56}$ is an isoleucine in D2R), whereas 5 differ in the D4R (see fig. S4). Qualitatively, this agrees with the finding that eticlopride, and some of its analogs, share similar affinities for the D2R and D3R with lower binding affinities for D4R. Mutation of four divergent residues in D2R to the aligned D4R residues led to a three-order-of-magnitude enhancement of binding to a D4R-selective antagonist (*34*). Most of the differences in ligand binding specificity between D4R and D2R/D3R can therefore be explained by the differences in physicochemical properties of the contact side chains, as the mutated D2 residues included three of the five nonconserved, eticlopride-contact residues—Val91$^{2.61}$Phe, Phe110$^{3.28}$Leu, and Tyr408$^{7.35}$Val.

The structural determinants of pharmacological specificity in the D3R and D2R are more subtle considering that the residues lining the binding pocket are essentially identical. In accordance with high conservation of the eticlopride binding site between D3R and D2R, the available structure-activity relationship (SAR) data suggest that, to achieve targeted selectivity (>100-fold), the ligand must extend toward the extracellular opening of the binding pocket [reviewed in (*12*)]. The D3R-selective pharmacophore consists of an extended aryl amide connected to an amine-containing scaffold by a relatively flexible four-carbon linker (fig. S1) (*35*). Previous

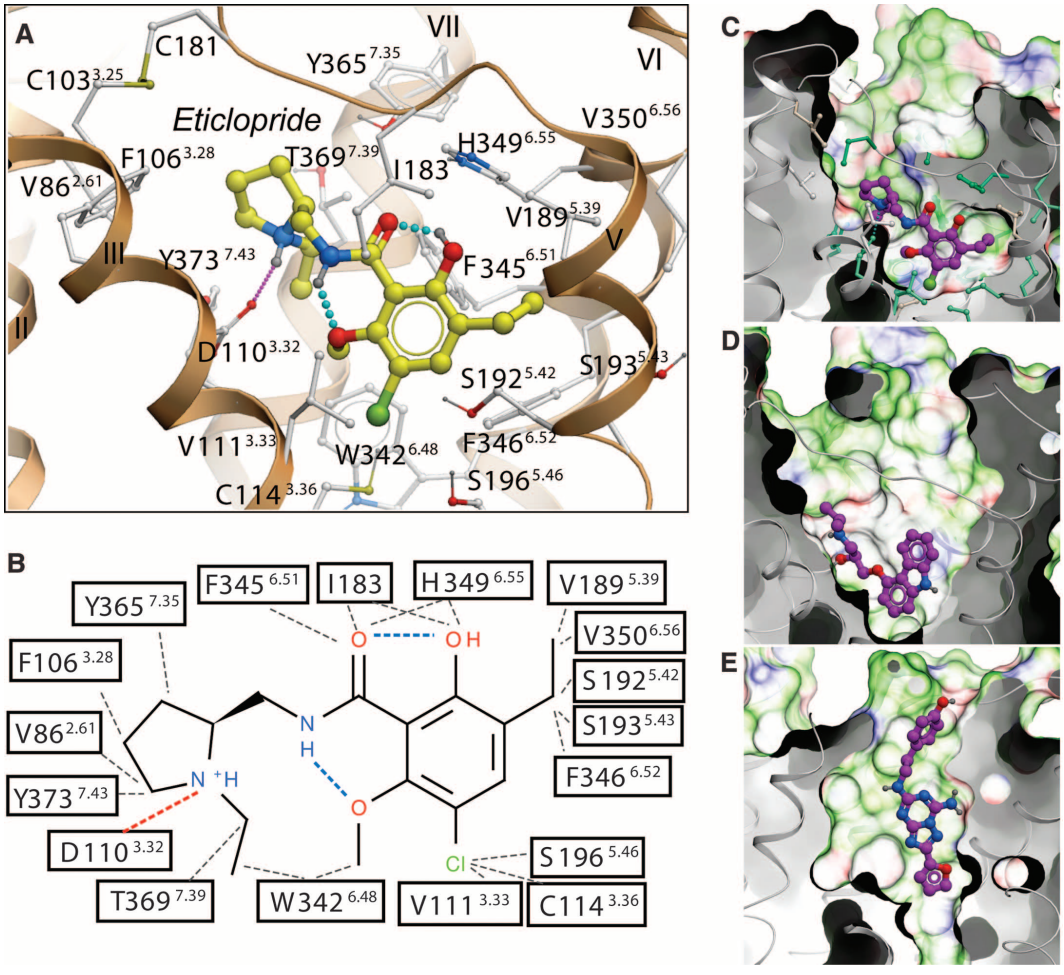

Fig. 3. Structural diversity of ligand binding sites in GPCR structures. (**A**) Close-up of the eticlopride binding site showing the protein-ligand interaction. (**B**) Chemical structure of eticlopride and interactions with the D3R residues; hydrophobic contacts are shown in gray dashed lines, hydrogen bonds in blue, and salt bridges in red. The ligand binding sites in (**C**) D3R, (**D**) β_2AR (PDB ID: 2RH1), and (**E**) A_{2A}AR (PDB ID: 3EML) crystal structures are shown in exactly the same orientation. A semitransparent skin shows the molecular surface of the receptor, colored by the residue properties (green, hydrophobic; red, acidic; and blue, basic). Corresponding ligands (C) eticlopride, (D) carazolol, and (E) ZM241385 are shown with carbon atoms colored magenta. For the D3R pocket, residues conserved between D3R and β_2AR are colored turquoise, and nonconserved residues are in gray.

efforts to rationalize the structural basis of D3R selectivity have naturally focused on regions that are not conserved, with primary attention being given to ECL2, which has previously been implicated in ligand binding to the D2R (*4*, *36*). Indeed, in chimeric studies, ECL2 has been found to play a role in both enantioselectivity and D3R selectivity of a number of compounds in which the butylamide linker is functionalized (*37*). In addition, roles for both ECL2 and ECL1 have been demonstrated for the D3R-selective tetrahydroisoquinoline, SB 269,652 (fig. S1) (*38*).

To explore the structural basis of selectivity, we created a homology model of D2R based on the D3R structure (*18*). Eticlopride could be reproducibly docked to the D3R structure and D2R model in orientations highly similar to that in the crystal structure. However, alignment of residues of the D3R and D2R indicates substantial differences in their extracellular electrostatic surfaces that could affect binding of other longer and bulkier ligands (figs. S5 and S6). Docking studies with the D3R-selective antagonist R-22 (*37*) revealed that the core amine-containing substituent (2,3-diCl-phenylpiperazine) binds in essentially the same binding pocket as eticlopride, whereas the indole-2-carboxamide terminus is oriented toward the extracellular part of the binding pocket consisting of ECL2/ECL1 and the junction of helices I, II, and VII, defining a second extracellular binding pocket (orange ellipse in Fig. 4A) that includes conserved Tyr373$^{7.43}$ and Glu95$^{2.65}$ (Fig. 4B). However, the residue at 1.39, which is spatially positioned between Tyr373$^{7.43}$ and Glu95$^{2.65}$, is divergent (Tyr36$^{1.39}$ in D3R and Leu41$^{1.39}$ in D2R) (Fig. 4, C and D). Moreover, Tyr36$^{1.39}$ is located in a stretch of five nonconserved residues at the extracellular end of helix I. Indeed, 44% of the extracellular half of helix I from 1.35 to 1.50 is not conserved between D2R and D3R (fig. S6), which should lead to functionally relevant changes in packing in D2R at the junction of helices I, II, and VII (Fig. 4, C and D, and fig. S7), consistent with previous structure-function investigations (*39*–*41*). The lack of conservation of Thr368$^{7.38}$ (Phe in D2R), which forms a hydrogen bond with the backbone of the conserved Tyr365$^{7.35}$ in the D3R, may also contribute to a shift in the relative position of helices I and VII (Fig. 4, C and D) (*42*).

Such differences in packing and backbone configuration between the D2R and D3R, even when relatively subtle, are expected to lead to changes in selectivity even without changes in ligand contact side chains in the binding pocket. Indeed, molecular dynamics simulations of the D2R in an explicit lipid bilayer (*18*) suggest a reorganization of ECL3 and helices I, II, and VII that alters the configuration of the second binding pocket (Fig. 4D and fig. S7). Accordingly, the distance between the conserved residues Glu95$^{2.65}$ (in the second binding pocket) and Tyr373$^{7.43}$ (between the orthosteric binding site and the second binding pocket) is ~1 Å greater in the D3R than in the D2R because of distinct 2.65-1.39-7.43 interactions (Fig. 4, C and D, and fig. S7), representing subtle but critical differences in the relative disposition between the orthosteric binding site and the second binding pocket in the D2R and D3R (Fig. 4B).

The crystal structure of the human D3R provides an opportunity to identify subtle structural differences, at the molecular level, between closely related GPCRs that can be exploited for novel drug design. In particular, the structural observation of an extracellular binding pocket, which may interact with bitopic or allosteric ligands, highlights the importance of the extracellular loops that were once thought to only provide superficial definition to ligand binding. Highly D2R and D3R subtype-selective molecules will provide the tools necessary to parse behavioral actions associated with individual subtypes and identify mechanisms underlying side effects, resulting in improved medications for the treatment of neuropsychiatric disorders, including drug abuse.

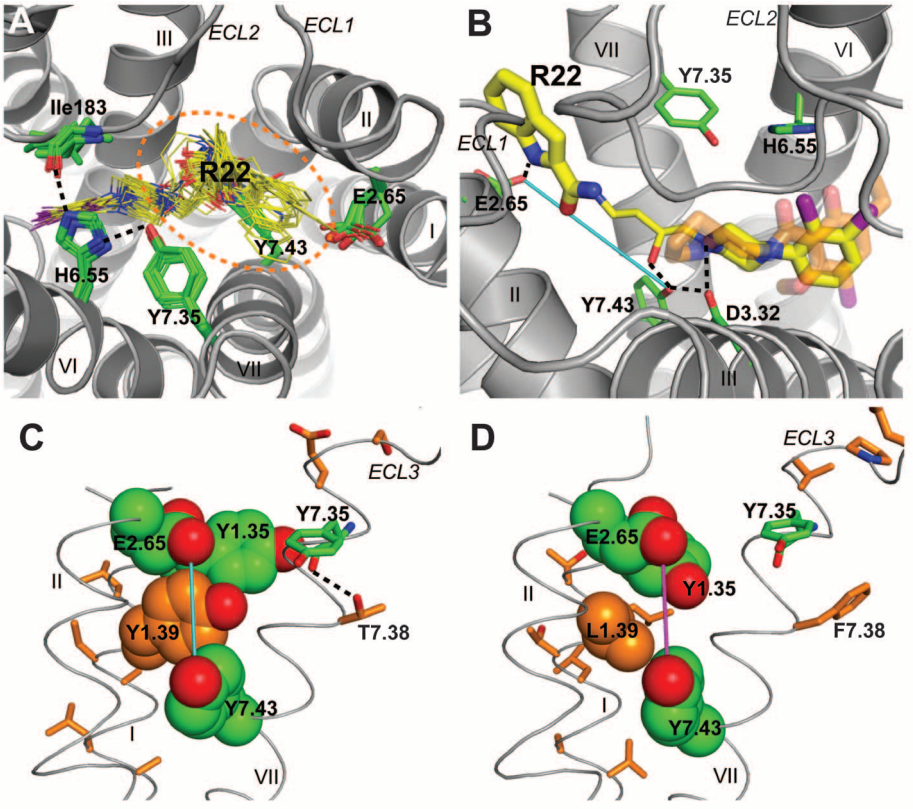

Fig. 4. The second binding pocket defined by R-22 is differentially modulated by nonconserved residues in D3R and D2R. (**A**) In addition to the core binding pocket, which essentially overlaps with that of eticlopride, the potential docking conformations of the core-constrained (see supporting online material) D3R-selective compound R-22 position the extended aryl amide within a second binding pocket comprising the junction of ECL1 and ECL2 and the interface of helices II, VII and I [dotted orange ellipse in (A)]. (**B**) In the docking pose with the most extended conformation of R-22 (yellow), the ligand makes contact with several key conserved residues, including Asp110$^{3.32}$, Tyr373$^{7.43}$, and Glu90$^{2.65}$. The linker region of R-22 connecting the aryl amide and phenylpiperazine moieties (see fig. S1) is in a thinner representation. The 2,3-diCl-phenylpiperazine occupies essentially the same space as bound eticlopride (orange). (**C** and **D**) Close-up view of the interface of helices II, VII, and I of the D3R (C) and D2R (D) showing the results of molecular dynamics simulations indicating that the nonconserved regions of helix I and position 7.38 (orange) may orient key conserved contact residues differently and alter the shape of the second binding pocket, as reflected by the simulated distances between Glu90$^{2.65}$ and Tyr373$^{7.43}$ in D3R (cyan) and D2R (magenta) (see fig. S7).

References and Notes

1. O. Civelli, in *Psychopharmacology: The Fourth Generation of Progress*, F. Bloom, D. Kufper, Eds. (Raven, NY, 1995), pp. 155–161.
2. B. Levant, *Pharmacol. Rev.* **49**, 231 (1997).
3. P. Sokoloff, B. Giros, M. P. Martres, M. L. Bouthenet, J. C. Schwartz, *Nature* **347**, 146 (1990).
4. L. Shi, J. A. Javitch, *Annu. Rev. Pharmacol. Toxicol.* **42**, 437 (2002).
5. P. Sokoloff *et al.*, *Eur. J. Pharmacol.* **225**, 331 (1992).
6. A. Holmes, J. E. Lachowicz, D. R. Sibley, *Neuropharmacology* **47**, 1117 (2004).
7. J. G. Gilbert *et al.*, *Synapse* **57**, 17 (2005).
8. M. Pilla *et al.*, *Nature* **400**, 371 (1999).
9. K. Spiller *et al.*, *Psychopharmacology (Berl.)* **196**, 533 (2008).
10. S. R. Vorel *et al.*, *J. Neurosci.* **22**, 9595 (2002).
11. Z. X. Xi *et al.*, *Neuropsychopharmacology* **31**, 1393 (2006).

12. C. A. Heidbreder, A. H. Newman, *Ann. N. Y. Acad. Sci.* **1187**, 4 (2010).
13. T. DePaulis, H. Hall, S. Ogren, *Eur. J. Med. Chem. Chim. Ther.* **20**, 273 (1985).
14. N. Griffon, C. Pilon, F. Sautel, J. C. Schwartz, P. Sokoloff, *J. Neural Transm.* **103**, 1163 (1996).
15. In Ballesteros-Weinstein numbering, a single most conserved residue among the class A GPCRs is designated x.50, where x is the transmembrane helix number. All other residues on that helix are numbered relative to this conserved position.
16. C. B. Roth, M. A. Hanson, R. C. Stevens, *J. Mol. Biol.* **376**, 1305 (2008).
17. D. M. Rosenbaum *et al.*, *Science* **318**, 1266 (2007).
18. Materials and methods are available as supporting material on *Science* online.
19. V. Cherezov *et al.*, *Science* **318**, 1258 (2007).
20. M. A. Hanson *et al.*, *Structure* **16**, 897 (2008).
21. V. P. Jaakola *et al.*, *Science* **322**, 1211 (2008).
22. T. Warne *et al.*, *Nature* **454**, 486 (2008).
23. J. M. Baldwin, *EMBO J.* **12**, 1693 (1993).
24. T. H. Ji, M. Grossmann, I. Ji, *J. Biol. Chem.* **273**, 17299 (1998).
25. A similar intraloop disulfide bond is present in the A_{2A}AR structure and likewise is thought to constrain the position of ECL3 and orients His359 at the top of the ligand binding site.
26. T. Okada *et al.*, *J. Mol. Biol.* **342**, 571 (2004).
27. K. Palczewski *et al.*, *Science* **289**, 739 (2000).
28. J. A. Ballesteros *et al.*, *J. Biol. Chem.* **276**, 29171 (2001).
29. R. Vogel *et al.*, *J. Mol. Biol.* **380**, 648 (2008).
30. R. O. Dror *et al.*, *Proc. Natl. Acad. Sci. U.S.A.* **106**, 4689 (2009).
31. E. V. Kuzhikandathil, L. Westrich, S. Bakhos, J. Pasuit, *Mol. Cell. Neurosci.* **26**, 144 (2004).
32. R. Duman, E. J. Nestler, in *Psychopharmacology: The Fourth Generation of Progress*, F. Bloom, D. Kupfer, Eds. (Raven, NY, 1995), pp. 303–320.
33. C. D. Strader *et al.*, *J. Biol. Chem.* **266**, 5 (1991).
34. M. M. Simpson *et al.*, *Mol. Pharmacol.* **56**, 1116 (1999).
35. F. Boeckler, P. Gmeiner, *Pharmacol. Ther.* **112**, 281 (2006).
36. L. Shi, J. A. Javitch, *Proc. Natl. Acad. Sci. U.S.A.* **101**, 440 (2004).
37. A. H. Newman *et al.*, *J. Med. Chem.* **52**, 2559 (2009).
38. E. Silvano *et al.*, *Mol. Pharmacol.* **78**, 925 (2010).
39. W. Guo *et al.*, *EMBO J.* **27**, 2293 (2008).
40. L. Shi, M. M. Simpson, J. A. Ballesteros, J. A. Javitch, *Biochemistry (Mosc.)* **40**, 12339 (2001).
41. G. L. Alberts, J. F. Pregenzer, W. B. Im, *Mol. Pharmacol.* **54**, 379 (1998).
42. J. A. Ballesteros, X. Deupi, M. Olivella, E. E. Haaksma, L. Pardo, *Biophys. J.* **79**, 2574 (2000).
43. This work was supported in part by Protein Structure Initiative (PSI) grant U54 GM074961 and PSI:Biology grant U54 GM094618 for structure production, NIH Roadmap grant P50 GM073197 for technology development, NIH grant R21 RR025336 (V.C.), and Pfizer. Additional support was provided by the National Institute on Drug Abuse Intramural Research Program (A.H.N.), grants DA022413 and MH54137 (J.A.J.), and grant DA023694 (L.S.). The content is solely the responsibility of the authors and does not necessarily represent the official views of the National Institute of General Medical Science or the NIH. We thank J. Velasquez for help with molecular biology, T. Trinh and K. Allin for help with baculovirus expression, D. Gray for assistance with eticlopride synthesis, M. Griffor for large-scale production of the receptor, X. Qiu for suggestions, and A. Walker for assistance with manuscript preparation. We acknowledge Y. Zheng, The Ohio State University and M. Caffrey, Trinity College (Dublin, Ireland), for the generous loan of the in meso robot (built with support from NIH grant GM075915), the National Science Foundation (grant IIS0308078), and Science Foundation Ireland (grant 02-IN1-B266); and J. Smith, R. Fischetti, and N. Sanishvili at the GM/CA-CAT beamline at the Advanced Photon Source, for assistance in development and use of the minibeam and beamtime. The GM/CA-CAT beamline (23-ID) is supported by the National Cancer Institute (grant Y1-CO-1020) and the National Institute of General Medical Sciences (grant Y1-GM-1104). Atomic coordinates and structure factors have been deposited in the Protein Data Bank with identification code 3PBL. A.H.N. is an inventor on a patent application from the National Institutes of Health that covers the use of R-22 and analogs as D3 receptor selective agents. R.C.S. is on the Board of Directors of Receptos, which does structure-directed drug discovery on GPCRs.

Supporting Online Material

www.sciencemag.org/cgi/content/full/330/6007/1091/DC1
Materials and Methods
Figs. S1 to S8
Tables S1 to S4
References

6 September 2010; accepted 21 October 2010
10.1126/science.1197410

Mcl-1 Is Essential for Germinal Center Formation and B Cell Memory

Ingela Vikstrom,[1] Sebastian Carotta,[1] Katja Lüthje,[1] Victor Peperzak,[1] Philipp J. Jost,[1] Stefan Glaser,[1] Meinrad Busslinger,[2] Philippe Bouillet,[1,3] Andreas Strasser,[1,3] Stephen L. Nutt,[1,3] David M. Tarlinton[1,3]*

Lymphocyte survival during immune responses is controlled by the relative expression of pro- and anti-apoptotic molecules, regulating the magnitude, quality, and duration of the response. We investigated the consequences of deleting genes encoding the anti-apoptotic molecules Mcl1 and Bcl2l1 (Bcl-x_L) from B cells using an inducible system synchronized with expression of activation-induced cytidine deaminase (Aicda) after immunization. This revealed Mcl1 and not Bcl2l1 to be indispensable for the formation and persistence of germinal centers (GCs). Limiting Mcl1 expression reduced the magnitude of the GC response with an equivalent, but not greater, effect on memory B cell formation and no effect on persistence. Our results identify Mcl1 as the main anti-apoptotic regulator of activated B cell survival and suggest distinct mechanisms controlling survival of GC and memory B cells.

Vertebrate immune responses are characterized by the clonal expansion of antigen-specific lymphocytes, by their differentiation into effector cells, and by the production of small, persistent populations of memory cells. An added feature of B cell immunity is the increasing affinity of the antibody response with time, with B cells expressing high-affinity antigen receptors (BCRs) preferentially recruited into the effector and memory compartments (*1*). The processes underpinning changes in affinity of immunoglobulin receptors occur within germinal centers (GCs), which are transient structures that arise after T cell–dependent immunization (*2*–*4*). Thus, the factors governing the survival of GC B cells will determine the qualitative and quantitative attributes of the effector cells—which in this case are plasma cells—and memory B cells. Survival of GC B cells is mediated by both the intrinsic and extrinsic apoptotic cell death pathways (*5*), with roles proposed for Fas ligand (CD95L)/Fas (CD95) (*6*, *7*), Bcl2l1 (Bclx$_L$) (*8*), Bcl2 (*9*, *10*), and Bim (*11*). These studies, however, do not identify the prosurvival molecules that are physiologically relevant within the GC.

To address the components of the intrinsic apoptotic pathway regulating GC B cell behavior, we first measured the expression of relevant proteins, comparing GC and follicular B cells (Fig. 1) (*12*). Besides Bcl2l1 and Bim expression being up-regulated and Bcl2 down-regulated as previously reported (*6*, *13*, *14*), Mcl1 protein was increased in GC B cells (Fig. 1).

Increases in Bcl2l1 and Mcl1 expression in GC B cells prompted us to examine the contribution of these prosurvival proteins to the production of memory B cells, plasma cells, and affinity maturation. We therefore conditionally deleted loxP-flanked alleles of *Bcl2l1* or *Mcl1* in B cells after antigen activation using a transgene-encoded Cre recombinase expressed concurrently with the activation-induced cytidine deaminase (*Aicda*) locus (*15*). The loxP-flanked alleles should therefore be deleted in B cells, initiating somatic hypermutation (SHM) or class-switch recombination (CSR), which are processes requiring activation-induced cytidine deaminase (AID) (*16*).

Bcl2l1$^{fl/-}$Aicda-Cre mice, with one *Bcl2l1* allele deleted (*17*) and one flanked by LoxP (fl) sites (*18*), were immunized with a T cell–dependent antigen composed of the 4-hydroxy-3-nitrophenyl (NP) hapten conjugated to keyhole limpet hemocyanin (NP-KLH). Cellular responses were analyzed 21 days later in *Bcl2l1$^{fl/-}$Aicda*-Cre and control mice, when GC and memory B cells coexist (*6*, *19*). No significant difference in the frequency or number of antigen-specific (NP^+IgG1^+) B cells was observed in the spleens of *Bcl2l1$^{fl/-}$Aicda*-Cre mice as compared with controls, both in total and after subdivision into GC ($CD38^-$) and memory ($CD38^+$) compartments (Fig. 2, A and B). Similarly, no differences were seen 7 and 14 days after immunization, excluding the possibility of an early deficit being masked by compensation as

[1]Walter and Eliza Hall Institute of Medical Research, 1G Royal Parade, Parkville, Victoria 3052, Australia. [2]Research Institute of Molecular Pathology, Vienna Biocenter, Dr. Bohr-Gasse 7, A-1030 Vienna, Austria. [3]Department of Medical Biology, University of Melbourne, Parkville, Victoria 3050, Australia.

*To whom correspondence should be addressed. E-mail: tarlinto@wehi.edu.au

Science
AAAS

Structure of the Human Dopamine D3 Receptor in Complex with a D2/D3 Selective Antagonist

Ellen Y. T. Chien *et al.*

Science **330**, 1091 (2010);
DOI: 10.1126/science.1197410

This copy is for your personal, non-commercial use only.

If you wish to distribute this article to others, you can order high-quality copies for your colleagues, clients, or customers by clicking here.

Permission to republish or repurpose articles or portions of articles can be obtained by following the guidelines here.

The following resources related to this article are available online at www.sciencemag.org (this information is current as of October 15, 2015):

Updated information and services, including high-resolution figures, can be found in the online version of this article at:
http://www.sciencemag.org/content/330/6007/1091.full.html

Supporting Online Material can be found at:
http://www.sciencemag.org/content/suppl/2010/11/17/330.6007.1091.DC1.html

A list of selected additional articles on the Science Web sites **related to this article** can be found at:
http://www.sciencemag.org/content/330/6007/1091.full.html#related

This article **cites 37 articles**, 14 of which can be accessed free:
http://www.sciencemag.org/content/330/6007/1091.full.html#ref-list-1

This article has been **cited by** 69 articles hosted by HighWire Press; see:
http://www.sciencemag.org/content/330/6007/1091.full.html#related-urls

This article appears in the following **subject collections:**
Biochemistry
http://www.sciencemag.org/cgi/collection/biochem

Downloaded from www.sciencemag.org on October 15, 2015

Science (print ISSN 0036-8075; online ISSN 1095-9203) is published weekly, except the last week in December, by the American Association for the Advancement of Science, 1200 New York Avenue NW, Washington, DC 20005. Copyright 2010 by the American Association for the Advancement of Science; all rights reserved. The title *Science* is a registered trademark of AAAS.